PART 3 – DETECTORS

Section

INTRODUCTION

Theory and state-of-the-art performance are given for radio and optical detectors.

Radio and optical detectors are considered in two major sections.

Radio Detectors

The normal figure of merit for radio detectors is the noise figure or noise temperature. These are documented as a function of frequency. Means of reducing the noise temperature of detectors by use of a low noise preamplifier is also quantitatively described.

Optical Detectors

Optical frequency detection falls into two general categories: that where heterodyne detection is required to obtain efficient detection and that category where direct detection will provide efficient detection. The latter is essentially limited to the visible light spectrum.

Operating theory is given for both categories as is measured performance.

SUMMARY OF DETECTION METHODS

Heterodyne performance for radio and optical frequencies is given. Optical heterodyne detection will probably find its greatest application in a wide band data link from a space probe. Direct detection is practical only at optical frequencies. It will probably find its greatest application as a beacon link to a deep space vehicle.

Heterodyne Detection

The performance of optical heterodyne detectors is similar to that of radio heterodyne systems but still differs markedly due to the high operating frequency. This has the effect of changing the dominant noise contribution from a spectral density given by kT (k is Boltzmann's constant and T absolute temperature) to a spectral density given by $h\nu$ where h is Plank's constant and ν is the operating frequency. In general, the noise power spectral density N increases with frequency.

Ideally,

$$N = \frac{h\nu}{e^{h\nu/kT} - 1} + h\nu$$

This curve is plotted as a function of frequency in the figure, for various noise temperatures, T_{in} °K. The figure compares detector performance over the radio-to-optical spectrum and shows the projected capability of optical detectors (using the above equation) in comparison with known radio receiver performance.

More recently heterodyne detectors have been constructed at both 3.39 microns[1] and 10.6 microns[2]. The performance of these detectors is much improved over that of the direct detector.

The radio frequency detectors indicated in the figure are of two types, a heterodyne mixer and a heterodyne mixer preceded by a low noise amplifier. When the gain of the amplifier is high its low noise characteristics become the dominant noise contribution of the detecting system.

Direct Detection

Direct detection is practical only for optical frequencies. In direct detection, the output signal is dependent only upon the input signal and background power. (No local oscillator power).

---

[1] Goodwin, F. E., "A 3.39 micron Infrared Optical Heterodyne Communication System," IEEE Journal of Quantum Electronics, QE-3, No. 11, pp. 524-531, November 1967.

[2] Goodwin, F. E., and Nussmeier, T. A., "Optical Heterodyne Communications Experiments at 10.6μ," Presented at International Quantum Electronics Conference, Miami, Florida, May 14-17, 1968.

Visible frequency detectors are largely of the direct detection type. These operate quite efficiently due to the relatively large photon energies at these frequencies.

The equation describing the signal-to-noise ratio for direct detection is:

$$\frac{S}{N} = \frac{\left(\frac{G\eta q}{hf} P_C\right)^2}{kTB_o G^2\left(\frac{\eta q}{hf} P_C + \frac{\eta q}{hf} P_B + I_D\right) R_L}$$

where:

G = detector gain

η = detector quantum efficiency

q = electronic change, 1.602×10^{-19} coulombs/electron

h = Plank's constant 6.624×10^{-34} watt sec. sec

f = light frequency, Hz

P_c = received carrier power, watts

R_L = load resistance, ohms

k = Boltzmann's constant, 1.38×10^{-23} watts/Hz °K

T = Amplifier noise temperature, °K

B_o = Amplifier bandwidth, Hz

P_B = Background received power, watts

I_D = dark current, amps

Symbolically this is

$$\frac{S}{N} = \frac{\text{Signal Power}}{\text{Thermal noise power} + \text{shot noise power} + \text{background noise power} + \text{dark current noise power}}$$

In any detector application it is necessary to evaluate this equation and adjust the parameters such that an adequate signal to noise ratio is obtained.

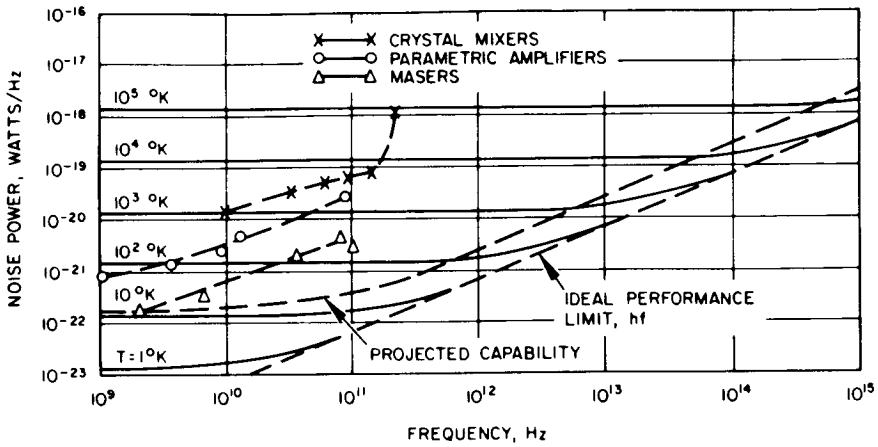

Heterodyne Receiver Noise Performance

DETECTORS

Radio Frequency Detectors

SENSITIVITY OF RF DETECTORS

Noise figures for crystal mixers, parametric amplifiers, and masers are given for microwave and millimeter wavelengths.

Detector or receiver sensitivity is conventionally characterized by the effective noise temperature, which is a measure of the receiver noise referred back to its input terminals, or by the noise figure, defined as

$$NF = \frac{S_{in}/N_{in}}{S_{out}/N_{out}}$$

The receiver noise temperature*, T_e, is related to the noise figure when the receiver is connected to a load at $0^{\circ}K$ by the expression

$$T_e = (NF-1)\, T_o$$

where T_o is a standard temperature taken to be $290^{\circ}K$.

The noise performance for several detector implementations is listed in this topic over a broad range of radio frequencies.

Micro/Millimeter-Wave Detectors

The more sensitive detection devices in this frequency range are the conventional crystal mixers, parametric amplifiers, and masers.

Crystal mixers are normally characterized by their conversion loss. The noise figure of the mixer is then

$$NF = L_C\, (NF_{IF} + N_R - 1)$$

where L_C is the conversion loss, NF_{IF} is the noise figure of the IF amplifier, and N_R is the crystal noise ratio. The conversion loss is defined as the ratio of RF input power to the measured IF output power at the mixer. The crystal noise ratio, N_R, is the ratio of noise power developed by the crystal to the thermal or Johnson noise of an equivalent resistance at $290^{\circ}K$ and is typically about 2 in a well-designed system. Estimates of best available noise performance from crystal mixers are summarized in the Table.

---

*Other system noise considerations are given in Volume IV, Part 1, "Background Radiation and Atmospheric Propagation."

Noise Performance for Radio Detectors

Noise Performance Estimates for Crystal Mixers

Frequency	Conversion Loss*	Noise Figure	Noise Temperature
10 GHz		6 db	870°K
35 GHz	5.5 db	10.3 db	2,800°K
60 GHz	6.5 db	11.3 db	3,600°K
94 GHz	8.2 db	12 db	4,300°K
140 GHz	9 db	13.8 db	6,700°K
200 GHz	19-20 db	25 db	91,000°K
300 GHz		35 db	910,000°K

*Where only conversion losses are quoted, i-f noise figure and crystal noise ratio are taken to be 2.

SENSITIVITY OF RF DETECTORS

Parametric amplifiers are generally available in the microwave range, but in the millimeter region availability is restricted to experimental models. Diode cutoff frequencies, associated with spreading resistances and junction capacitances, prevent the practical extension of operation beyond 100 GHz except by direct insertion of the diode into a cavity.

Masers are available in the microwave range. As is the case for parametric amplifiers, operation at millimeter wavelengths has been restricted to experimental models. Representative values of the best noise performance at several frequencies are also given in the Table.

Hot carrier detectors are based on the application of microwave power to a noninjecting point contact. As the majority carriers are excited, a temperature gradient between the point contact and broad contact is established, and a unidirectional thermoelectric voltage is generated with frequency following as high as 100 GHz. Work[1] on these detectors is in the experimental stage.

Submillimeter-Wave Detectors

The mechanisms for detection of submillimeter radiation are based on either a thermal effect or a photoelectric effect. Since thermal response times are generally long (in the millisecond range), applications to high-data-rate communication systems are limited to detectors utilizing photoelectric mechanisms. In general, these devices must be cooled to reduce thermal lattice vibrations so that only electrons absorbing the low electron energy (1.2×10^{-3} ev for $\lambda = 1$ mm) are excited to the conduction band. Detection has been demonstrated using several semiconductor materials, and a superconductive detector based on electron tunneling has been proposed.[2] In addition, detection of submillimeter and millimeter waves by down-conversion to the microwave region has recently been proposed and analyzed.[3] At present, however, definitive data are not generally available on detectors in the submillimeter region.

---

[1] Harrison, R. I. and Zucker, J., "Hot-Carrier Microwave Detectors," Proc. IEEE 54, pp. 588-595, 1966.

[2] Shapiro, S. and Jonus, A. R., "RF Detection by Electron Tunneling between Super Conductors," Proc. 8th International Conf. on Low Temperature Physics., pp. 321-323, Butterworth, London, 1962.

[3] Krumm, C. F. and Hadded, G. I., "Millimeter- and Submillimeter-Wave Quantum Detectors," Proc. IEEE 54, pp. 627-632, 1966.

Noise Performance for Radio Detectors

State-of-the-Art Performance of Parametric Amplifiers

Frequency	Noise Figure
1 GHz	0.8 db
3 GHz	1.3 db
9 GHz	2 db
14 GHz	3.5 db
94 GHz (estimated)	10 db

State-of-the-Art Performance of Masers

Frequency	Noise Temperature
2 GHz	10-15°K
8 GHz	20-25°K
35 GHz	130°K
81.3 GHz	300°K
94 GHz	200°K

RADIO FREQUENCY AMPLIFIERS

Masers and helium cooled paramps are the best candidates for a very low noise earth receiving station.

There are five low-noise microwave amplifiers which may be considered for use in a deep space communication system. These are

- Transistor Amplifier
- Tunnel Diode Amplifier (TDA)
- Traveling Wave Tube (TWT)
- Parametric Amplifier
- Maser

Brief discussions of the characteristics of these amplifiers are given in the following paragraphs:

Transistor Amplifiers

Microwave transistor amplifiers are relatively new devices which have promise of moderately low noise figures. At the present time noise temperatures of 200 to 625°K can be obtained at frequencies up to about 1 GHz with approximately 20 db gain. It is estimated that in ten years 120° to 170°K noise temperatures are likely at 2 GHz and feasible up to 15 GHz. Transistor amplifiers appear to have their most useful application as a second stage amplifier following an ultra low noise amplifier.

Tunnel Diode Amplifiers

The tunnel diode amplifier (TDA) is the simplest solid-state microwave amplifier and has moderate gain and noise characteristics. Noise temperatures range from about 360°K at 1 GHz to 520°K at 10 GHz using gallium antimonide diodes. Germanium diodes have about 1 db higher noise figures but are available for operation up to about 20 GHz. Single stage amplifiers normally provide about 17 db gain. However, stable gains as high as 30 db can be obtained by careful attention to temperature control and power supply stability. Bandwidths are more than adequate for space communication systems. Noise figures of room temperature TDA's are not expected to improve significantly. Such TDA's will, therefore, be of use mainly as second stage devices following ultra-low noise amplifiers when high noise performance is required.

The noise generated by a tunnel diode amplifier is largely caused by shot noise from the diode bias current. The magnitude of this noise contribution is determined by the characteristics of the material used and can be reduced by using low energy gap materials such as indium antimonide. Such materials must be operated at cryogenic temperatures. However, assuming that a suitable material can be found, a cryogenic TDA with a noise temperature of 20°K at 1 to 2 GHz would have a strong advantage over cooled paramps and masers in that no pump power would be required. A tunnel diode amplifier is shown in Figure A.

Traveling Wave Tubes

These devices offer high gain and moderately low noise figures. Noise temperatures in the 360 to 440°K range are presently obtainable over narrow bandwidths up to 2 GHz. It is unlikely that noise temperatures below about 225°K will be consistently obtained in the next decade. The two major noise sources in a TWT are beam shot noise and thermal noise from the attenuator. Present low noise TWT designs require complex anode structures to achieve space charge smoothing for shot noise reduction. Since no significant advances in space charge smoothing have been made since the late 1950's, it is not anticipated that major progress will be made within the next decade. Some improvement in noise temperatures can be expected by cooling the attenuator, but it does not appear that TWT's will be competitive with cooled paramps.

Parametric Amplifiers

Parametric amplifiers have demonstrated room temperature noise performance superior to that of transistor and tunnel diode amplifiers and cryogenic noise performance approaching that of the maser. In recent years the uncooled parametric amplifier has achieved a level of reliability that has permitted applications on a broad basis and in large numbers. Noise temperatures range from about 60°K at 1 GHz to 250°K at 10 GHz for well-designed narrow band amplifiers.[1] When cooled to 20°K, noise temperatures between 14°K at 1 GHz and 30°K at 10 GHz are possible with careful design using presently available components. Narrow band gains as high as 30 db are possible using extremely stable temperature and pump power control. Major advances for the cooled paramp are likely to be in cost reduction and reliability particularly in the associated cryogenic equipment. A paramp is shown in Figure B.

Masers

Masers find applications in special areas where the ultimate in low noise performance is either dictated by technical requirements or provides the most economical solution to the problem. The noise temperature of the maser itself is approximately that of its physical temperature, about 50°K. To this must be added the noise contribution of the section of input transmission line over which the temperature transition to room temperature is made. For frequencies in the range 1 to 20 GHz this contribution can be held to 5 to 10°K giving an overall maser noise temperature of 10 to 15°K. Gains of better than 30 db with bandwidths of 1 to 2 MHz or more are readily obtainable with a cavity maser. The major disadvantage of masers is that they must operate at a temperature of a few degrees Kelvin in order to provide sufficient gain. The complexity and cost of a cryogenic system increases rapidly as the temperature approaches 0°K.

Future improvements in the maser are likely to be in the area of reliability and cost reduction.

---

[1] Matthei, W. G., "Recent Developments in Solid-State Microwave Devices," The Microwave Journal, 9, No. 3, pp. 39-47, March 1966.

RADIO FREQUENCY AMPLIFIERS

Summary

A summary of the important properties of low noise amplifiers is given in the Table. Of the devices surveyed, only the maser and helium cooled paramp can presently meet the low-noise temperature requirements for the down-link receiver in a deep-space communication system, and a system based on reasonable extensions of today's state of the art would require one of these two devices. A suitable maser requires a physical temperature of 4.2°K or less while the paramp can provide adequate noise performance at physical temperatures up to 20°K. It follows that the cryogenic system for the paramp would be considerably less complex and less expensive. Barring the discovery of new types of ultra low noise amplifiers, the helium cooled parametric amplifier operating at 20°K presently appears to provide the most economical solution. Transistor and tunnel diode amplifiers could be used as low noise second stage devices.

Low Noise Preamplifier Characteristics

Amplifier Type	Gain Per Stage, db	Coolant Temperature °K	Relative Cost (1975-1980)	Relative Reliability (1975-1980)	Present Noise Temperatures (Amplifier Only), °K			Estimated Best Noise Temperature (1975-1980) (Amplifier Only), °K		
					Frequency, GHz			Frequency, GHz		
					1	2	10	1	2	10
Traveling Wave Tube	35	290	Medium to High	Medium	380°	400°	1340°	225°	250°	350°
Tunnel Diode Amplifier	20	290	Low	High	360°	380°	625°	310°	330°	500°
	20	20	Medium to Low	Medium	225°*	225°*	525°	200°†	250°†	350°†
Transistor Amplifier	20	290	Low	High	200°	625°	---	75°	125°	170°
Parametric Amplifier	20	290	Medium	High	60°	80°	250°	30°	40°	130°
	20	20	High	Medium	18°	20°	50°	15°	15°	20°
Maser	30	4.3	Very High	Low	10-15°	10-15°	10-15°	12°	12°	12°

*Estimate based on use of indium antimonide tunnel diode at 77°K
†Feasibility not established

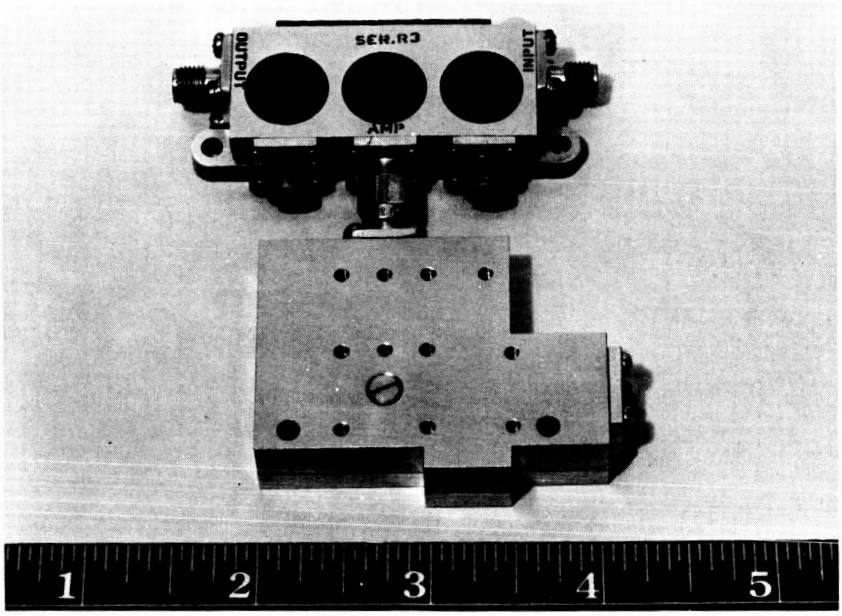

Figure A. Tunnel Diode Amplifier.

(The amplifier is encompassed by isolators – dark circles – and attached to a power supply)

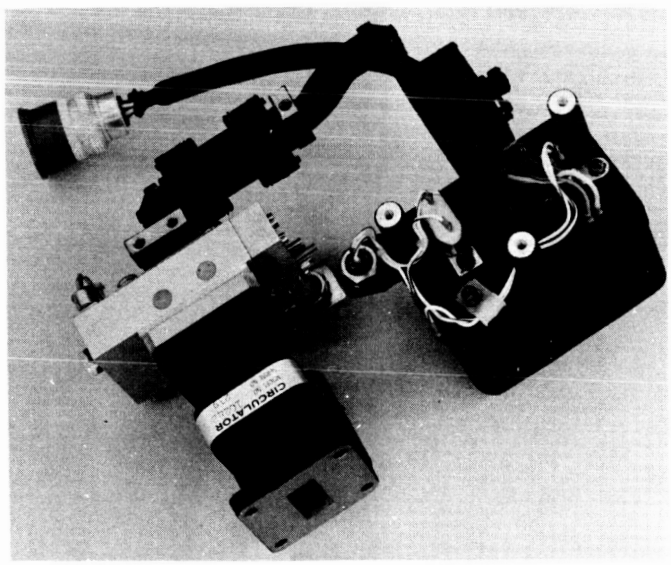

Figure B. Parametric Amplifier – Paramp.

(The amplifier is driven at a frequency higher than the one amplified. The source for this is the dark enclosure to the right of the picture. The paramp proper is housed in the light colored enclosure.)

DETECTORS

Optical Frequency Detectors

INTRODUCTION

Two general implementations for optical detectors are of concern in laser communications, photomultiplier detectors, used in the visible and near visible portion of the spectrum, and semiconductor devices used in the visible and in the infrared.

The material in this sub-section is concerned with two types of optical detection, that done using photomultipliers and that done using semiconductor photodiodes. Immediately following these topics, are topics dealing with the theory of operation of these detectors. Following the theory are topics which give present implementations of these types of detectors.

The final group of topics in this subsection deals with the relations of these detectors to their weight and cost. These burden relationships are to be used in the optimization of space communications systems described in Volume II, Part I of this final report.

Detectors may be used as direct detectors (those where the output is dependent only upon the signal input) or heterodyne detectors (where the output signal is dependent both upon the input signal and upon a local oscillator). Visible frequency detectors are largely of the direct detection type. These operate quite efficiently due to the relatively large photon energies at these frequencies.

More recently heterodyne detectors have been constructed at both 3.39 microns[1] and 10.6 microns[2]. The performance of these detectors is much improved over that of the direct detector.

The performance of optical heterodyne detectors is similar to that of radio heterodyne systems but still differs markedly due to the high operating frequency. This has the effect of changing the dominant noise contribution from a spectral density given by kT (k is Boltzmann's constant and T absolute temperature) to a spectral density given by hf where h is Plank's constant and f is the operating frequency. In general, the noise power spectral density, N, increases with frequency.

Ideally,

$$N = \frac{hf}{e^{hf/kT} - 1} + hf$$

This curve is plotted as a function of frequency in the figure, for various noise temperatures, $T_{in}{}^{o}K$. The figure compares detector performance over the radio-to-optical spectrum and shows the projected capability of optical detectors (using the above equation) in comparison with known radio receiver performance.

[1] Goodwin, F. E., "A 3.39 micron Infrared Optical Heterodyne Communication System," IEEE Journal of Quantum Electronics, QE-3, No. 11, pp. 524-531, November 1967.

[2] Goodwin, F. E. and Nussmeier, T. A., "Optical Heterodyne Communications Experiments at 10.6μ," presented at International Quantum Electronics Conference, Miami, Florida, May 14-17, 1968.

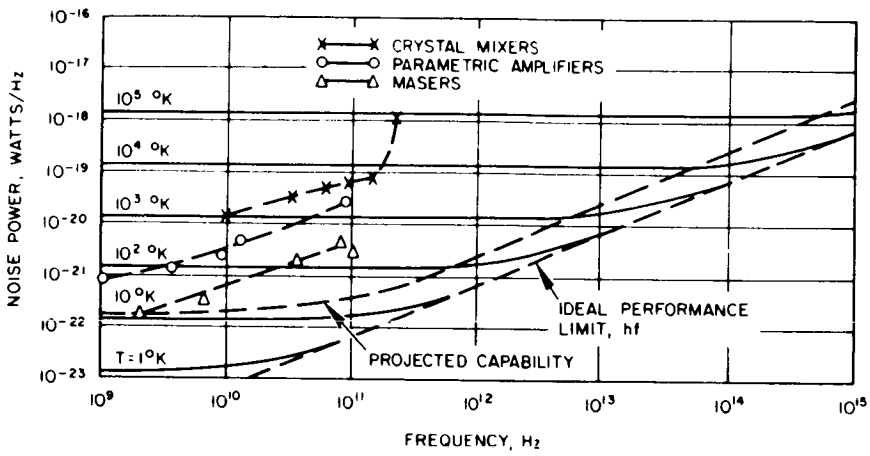

Heterodyne Receiver Noise Performance

CHARACTERIZATION OF OPTICAL DETECTORS

Optical detector performance can be described by certain photon input-electrical output response characteristics such as Responsivity; Detectivity, D*; and NEP.

The detectivity, D, is a quantitative measure of the relative performance of a receiver in terms of the signal-to-noise ratio of the detector under a specified level of irradiation.

The responsivity as defined by

$$R(\lambda) = \frac{S(\lambda)}{P(\lambda)}$$

where

$S(\lambda)$ = electrical output of detector at wavelength λ

$P(\lambda)$ = rms value of the incident power at wavelength λ

If $N(\lambda)$ is the receiver noise power, the detectivity is given, in terms of the responsivity by

$$D(\lambda) = \frac{R(\lambda)}{N(\lambda)}$$

A common figure of merit for detector is the noise equivalent power, NEP, given by

$$NEP = {}^{1}/_{D}$$

Semiconductor infrared detectors generally have detectivities that vary with bandwidth as $(\Delta f)^{-1/2}$ and with sensitive area as $A^{-1/2}$. A specific detectivity D* is then defined by the relation

$$D^* \equiv D(\lambda, f) = D\sqrt{(A)(\Delta f)}$$

where λ is the optical wavelength where D* is measured and f is the frequency at which D* is measured.

THEORY OF PHOTOMULTIPLIER DETECTORS

Photomultiplier detectors operate best at visible frequencies where the incoming photon energy is large enough to overcome the work function of the surface and cause electron emission.

The most useful lasers for optical communications systems are found in the wavelength region from 0.4 to 10μ; i.e., from the visible through the near infrared region of the spectrum. A variety of detection mechanisms and devices have been used in this spectral region, but not all are useful for the contemplated systems applications. Thermal detectors, for example, are much too slow, having time constants no shorter than several milliseconds, and their use is generally restricted to spectroscopy and energy reference measurements. Detectors based on mechanisms in which the energy of the absorbed photon goes into direct electronic excitation of the material are much more useful where fast response is required. These include the photo-emissive detectors generally used in the visible and the semiconductor devices applied in the infrared and visible. This topic will be limited to photo emissive detectors while the following topic deals with semiconductor devices.

In the visible and near-infrared region of the spectrum, the photomultiplier is the most efficient and convenient detector of radiation. It is based on the external photoelectric effect and the subsequent amplification of the electron current by means of a number of secondary emitting stages termed "dynodes." The basic and determining process in the photomultiplier is the external photoelectric effect, which consists of two steps: absorption of light by a solid and emission of an electron.

Electron emission will take place only when a photon possesses sufficient energy to overcome the work function of the solid, i.e., when

$$h\nu \geq e\Phi$$

where e is the electronic charge and Φ is the work function. This relation sets a long wavelength limit for every photoemissive detector; it may be put in the form

$$\lambda_L = \frac{1.24}{e\Phi}$$

where λ_L is the wavelength limit in microns and $e\Phi$ is the work function of the photocathode in electron volts.

The element with the lowest work function is cesium. For this element $e\Phi = 1.9$ eV; therefore, the wavelength limit of a cesium photocathode is about 6500 Å. Composite photocathodes consisting of combinations of metals and oxides have lower work functions; they are capable of functioning up to about $\lambda = 1.2\mu$. Naturally, as the limit is approached the efficiency of the detector decreases. The variation of detector efficiency with wavelength is apparent from the responsivity curves or the curves of quantum efficiency, which in the case of photoemissive detectors are simply related to the responsivity curves.

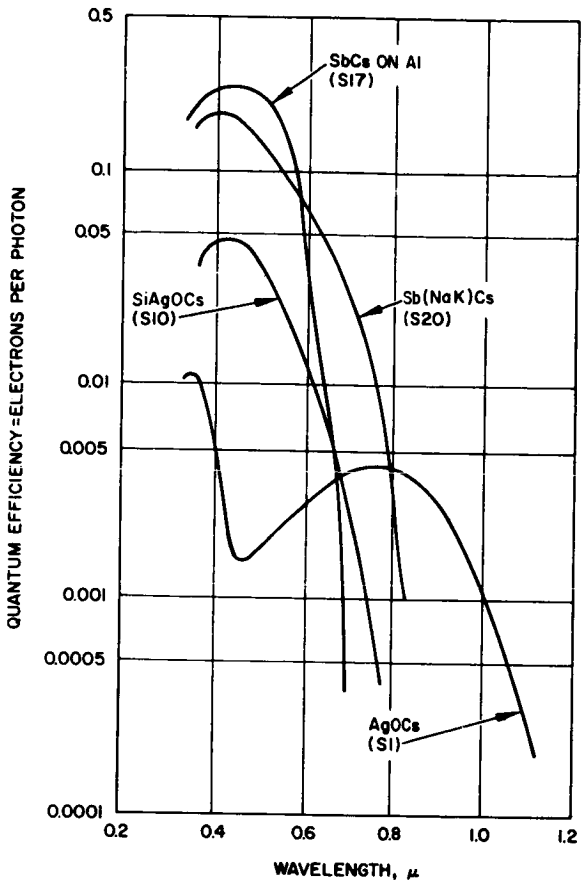

Figure A. Spectral Response of Various Photocathodes

THEORY OF PHOTOMULTIPLIER DETECTORS

Quantum efficiency, η, is the number of emitted electrons divided by the number of incident photons. The frequency, ν, quantum efficiency, η, incident power, P, and the photoelectric current, i, are related as follows: The number of incident quanta per second is $n = P/h\nu$, the electron current emitted from the photosurface is ηne; therefore

$$i = \eta e \, P/h\nu$$

Responsivity $R(\nu)$ is proportional to i/P; therefore

$$R(\nu) = \frac{Ge\eta \ (\nu)}{h\nu}$$

where G is the gain of the photomultiplier. The quantum efficiencies, $\eta(\nu)$, of the red-sensitive photocathodes are shown as a function of in Figure A.

As a circuit element, a photomultiplier appears simply as a capacitance in parallel with a current generator of magnitude $i = Ge\eta \ P/h\nu$, as in Figure B.

In the photomultiplier there is shot noise due to the fluctuations in the mean dc current. This current is the sum of dark currents that flow in the absence of any light input and the average photocurrent due to both signal and extraneous optical inputs. These sources together contribute a white noise power spectrum with a circuit representation as a current generator with a mean square amplitude (Figure C).

$$\overline{i^2_{nd}(f)} = \left(2eI_d + 2e^2\eta \frac{Pav}{h\nu} G\right) \Delta f$$

I_d is the dark current and Pav the average incident optical power. There will also be a noise contribution from the resistive part of the equivalent load R_L whose magnitude is

$$i^2_{nr}(f) = \frac{4kT_e}{R_L} \ \Delta f$$

T_e is an effective temperature used to characterize the noise performance of the receiver. Photomultiplier detectivity is given by:

$$D = \frac{Ge\eta}{h\nu} \frac{1}{\left[2eI_d + 2e^2\eta \left(P_{av}/h\nu\right) G + \left(4kT_e/R_L\right)\right]^{1/2} (\Delta f)^{1/2}}$$

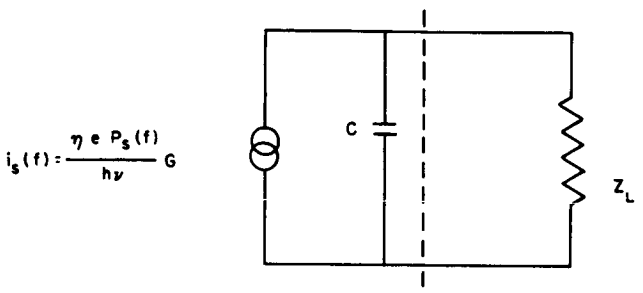

Figure B. Signal Equivalent Circuit of Photomultiplier

THEORY OF PHOTOMULTIPLIER DETECTORS

The response times of ordinary photomultipliers are between 1 and 3 nsec. The responsivity is fairly uniform until the frequency $f = 1/2\pi\tau$ is reached. Thus the performance of the commercial photomultipliers begins to be degraded between 50 and 150 MHz modulation frequency. Special tubes are required for the detection or demodulation of signals varying faster rates.

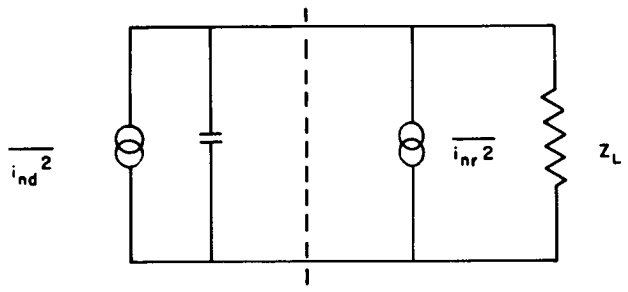

$$\overline{i_{nd}^2} = (2eI_d + 2e^2\eta\frac{P}{h\nu}G)\Delta f$$

$$\overline{i_{nr}^2} = \frac{4k\,T_e\,\Delta f}{R_L}$$

Figure C. Noise Equivalent Circuit of Photomultiplier

SOLID STATE DETECTORS OPERATING CONCEPTS

Photoconductive, photoelectromagnetic, and photovoltaic modes of detection are described.

The treatment of the various internal photoeffects in semiconductors can be presented in a unified fashion. Therefore both intrinsic and extrinsic mechanisms will be discussed in this topic.

At wavelengths greater than 1.1μ, photoemissive devices no longer have sufficient sensitivity and detectors utilizing internal photoeffects must be employed. Solid state detectors with detectivities approaching the theoretical photon noise limit in the wavelength range 0.4μ to 10μ are available as a result of the considerable progress in infrared technology in the past decade.

There are two internal photoeffects which are the basis of solid state detectors operating in the near infrared. In both cases, absorption of photons leads to a change in the concentration of free, mobile charge carriers within the material. In the first class of detectors, called intrinsic, the energy of an absorbed photon creates an electron-hole pair, i.e., the excitation process raises an electron from a valance band state to a conduction band state and only photons with energies greater than the intrinsic band gap are effective. The excitation process in the second class of detectors, called extrinsic, is the ionization of an impurity center to produce a free carrier and a charged defect site. The optical absorption constant in intrinsic materials is large, ranging up to 10^5 cm^{-1}, whereas in extrinsic materials it is rarely greater than 10^2 cm^{-1}. Photogenerated carriers are therefore confined to much smaller regions of intrinsic detectors.

In intrinsic detectors there are three commonly used techniques for sensing the rate at which electron-hole pairs are generated by the incident light. These are the photoconductive, the photoelectromagnetic, and the photovoltaic modes of operation.

Figure A-1 represents a detector operated in the photoconductive mode. The dashed line represents the steady state electron-hole concentration in a uniform block of material. The current that flows in response to an electric field applied between the electrodes provides a measure of the free carrier concentration. When signal photons are incident on the detector, an additional concentration of carriers is set up which varies with position in the detector as shown by the solid curve. Because of the additional carriers a larger current flows in the external circuit.

The photoelectromagnetic mode of operation is obtained if the electric field is removed from the photoconductor so that it is connected directly across a load and a magnetic field is applied perpendicular to the plane of the figure. Because of the concentration gradient of electron-hole pairs produced by the absorbed radiation in the material, carriers drift in the direction in which radiation is incident. The Lorentz force due to the magnetic field on the moving carriers deflects the electrons and holes to opposite electrodes and produces current in the external load as illustrated in Figure A-2.

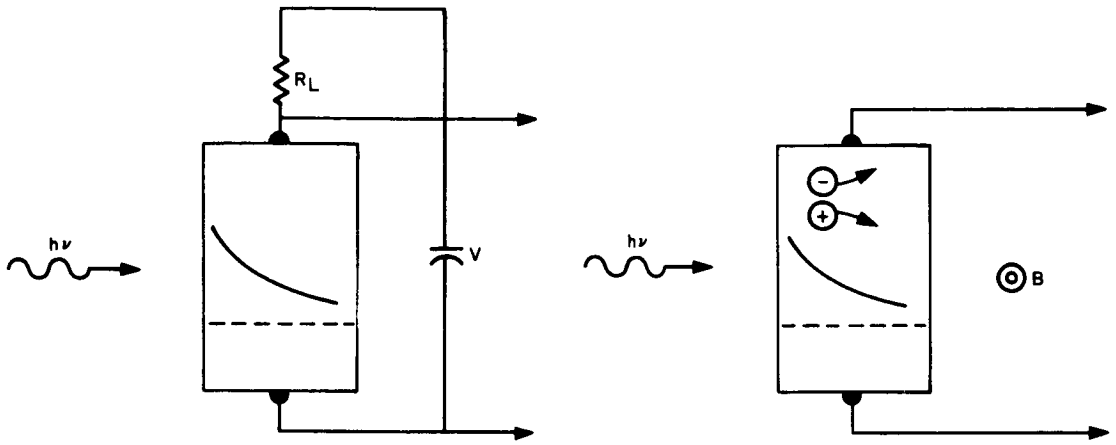

1) Photoconductive Mode

2) Photoelectromagnetic Mode

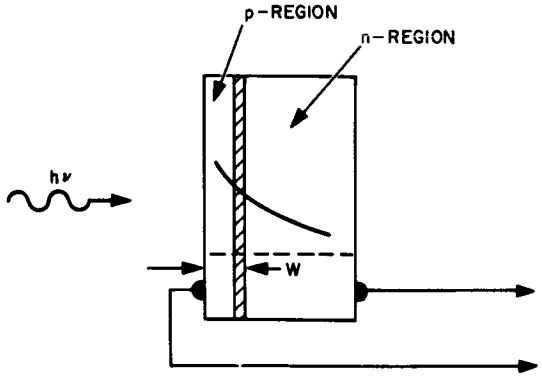

3) Photovoltaic Mode

Figure A. Three Modes of Operation of Solid State Photodetectors

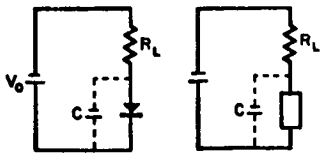

Figure B. Operating Circuits of Photodiode and Photoconductor Detectors

SOLID STATE DETECTORS OPERATING CONCEPTS

The third mode of operation is the photovoltaic mode in which a p-n junction is produced immediately behind the surface on which radiation is incident by diffusing a p-type dopant into n-type material (Figure A-3). The generated electron hole pairs diffuse to the junction under the influence of the concentration gradients set up in response to the incident radiation. The electric fields in the junction drive the electrons to the n-side and holes to the p-side of the detector. With zero applied bias, an external photocurrent can be observed or the detector may be operated with reverse bias in what is essentially a photoconductive mode.

By appropriate control of the fabrication process, it is possible in some semiconductors to make the transition region between the n and p regions large or even to arrange that the detector consist of three regions: a thick n-type base region on which there is first a moderately thick intrinsic region, and then a very thin p region at the surface on which radiation is incident. Such a p-i-n structure has somewhat different response time characteristics when biased in the reverse direction and is particularly useful for weakly absorbed radiation.

Typical circuits in which the reverse biased photodiode and the photoconductor are operated are shown in Figure B. The load resistor R_L represents the input resistance of the amplifier, and C includes all shunt capacities in the input circuit. The current-voltage characteristics of these two devices are represented schematically in Figure C for various incident photon fluxes. The direction of the arrow indicates increasing incident flux.

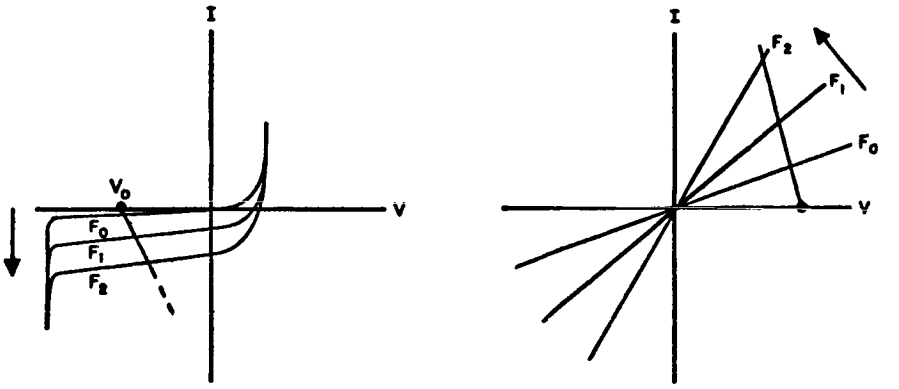

Figure C. Representative Current-Voltage Characteristics of a Photodiode (left) and a Photoconductor (right) for Various Values of Incident Flux

Arrows indicate directions of increasing flux, i.e., $F_2 > F_1 > F_0$.

DETECTION LIMITS OF SOLID STATE DETECTORS

Signal to noise ratios are derived for solid state detectors considering the various types of noises which may be present.

The constant current equivalent input circuits for photodiode and photoconductor detectors are shown in Figure A. They are identical except for the inclusion of the series resistance R_s in the diode circuit. R_s is usually of the order of a few ohms for most well made diodes and so is negligible except for extremely high frequency operation.

Current flows in the detector circuits in response to the incident photon fluxes. In the diode each generated electron-hole pair results in the traversal of the external circuit by an elementary charge. For the photoconductor, the generated free carriers contribute to the external current only for a mean time, τ, their lifetime. Lifetime effects may reduce the response of a diode, but the fast diode can be designed to minimize this effect. The constant current generators in the equivalent circuits of Figure A accordingly provide currents given by

$$I = I_{dc} + i_s(\omega) = e\eta M(F_B + F_{Lo} + F_{so}) + e\eta M F_{so} S(\omega) e^{j\omega t}$$

When I_{dc} is the direct current

$i_s(\omega)$ is the frequency dependant current

e is the electronic charge

η is the quantum efficiency

M is the diode multiplication factor

F_B is the background photon flux

F_{Lo} is the laser local oscillator photon flux

F_{so} is the signal photon flux

$S(\omega)$ is the frequency degradation due to transit time and lifetime effects.

This expression is applicable to both the diode and the photoconductor. In the ordinary diode the factor M is always equal to unity; when an avalanche diode which provides internal gain through impact ionization is used, M is the multiplication factor of the diode. In the photoconductor, $M = \tau/\tau_R$, where τ is the lifetime of the free carriers and τ_R is their transit time (i.e., the time required for a free carrier to traverse the distance between the contacts on the device). The quantity τ_R is given by $L^2/\mu V$ where L is the length of the detector in the direction of current flow, μ is the mobility of the free carriers, and V is the bias voltage applied across the detector. Note that $V/L = E$, where E is the electric field intensity in the sample.

$S(\omega)$ is a frequency dependent term that gives the degradation of the detector response as a result of lifetime and carrier transport time effects. Its form for the diode can be quite complicated, depending on its detailed construction. However, it quite generally indicates that the response drops at frequencies so large that $\omega\tau_R \geq 1$. For the photoconductor, where it results from the finite lifetime of the carriers, it has the form $S(\omega) = (1 + j\omega t)^{-1}$.

In addition to the currents, which are caused by photons incident on the detector, internal currents may be present which would flow even if the detector were in a thermal equilibrium environment with no external incident radiation. In diodes there will be the usual reverse saturation currents and in some cases leakage currents around the junction region. For the photoconductor, leakage currents are possible under low background conditions where sample impedances would be large. Thermally generated currents will appear if the detector operating temperature is too high. Although such currents will not affect the signal currents at frequency, ω, they must be considered as possible sources of undesirable noise.

Noise at the signal frequency will arise from a number of sources in the detector and its associated circuitry. A basic noise source, over which there is no possibility of control through circuit design or detector fabrication techniques, is fluctuations in the photon-induced currents. In the diode this noise is referred to as shot noise and in the photoconductor as generation-recombination (g - r) noise. The mean power spectrum for this noise can be represented by

$$\overline{i^2(\omega)} = 2eM_n I_{dc}$$

for both structures. M_n is 1 for the diode and is $2(\tau/\tau_R)$ for the photoconductor. It should be noted that M_n does not have the same values for different types of detectors. I_{dc} includes both internally generated and photon generated currents.

A second type of noise whose effects can usually be minimized by appropriate circuit design is the thermal equilibrium Nyquist noise arising in the resistive components in the input circuits. When extremely wide bandwidth operation is required, Nyquist noise usually determines the performance limits of the detector.

In addition to these two unavoidable noises, practical detectors and amplifiers exhibit excess noises that are difficult to control and whose sources may not even be well understood. The $1/f$ noises found at low frequencies in almost all semiconductor devices are included in this group, as are the excess noises arising in preamplifiers. Since $1/f$ noise in the detectors can usually be made negligible above at least a few kilocycles by proper fabrication techniques, this noise source will be neglected in the following treatment. Excess noises arising in the preamplifier will also be neglected for the sake of clarity. Only shot, generation-recombination, and Nyquist noise will be considered of further.

DETECTION LIMITS OF SOLID STATE DETECTORS

The noise equivalent circuit for the diode and the photoconductor is shown in Figure B. For this circuit the noise current power spectrum is given simply by

$$\overline{i_n^2(\omega)} = 2eI_{dc} \left|S(\omega)\right|^2 + 4kT/R_p$$

or more explicitly by

$$\overline{i_n^2(\omega)} = 2eI_i M_n \left|S(\omega)\right|^2 + 2e^2\eta M M_n (F_B + F_{Lo} + F_{so}) \left|S(\omega)\right|^2 + 4kT/R_p$$

where

k is Boltzmann's constant

T is absolute temperature

R_p is the parallel resistance of the detector and load

I_i is internal current

where the internal currents and the photon generated currents have been written explicitly. F_B represents the background photon flux. The significance of the M factor is:

$M = 1$ ordinary diode

$= \tau/\tau_R$ photoconductor

$M_n = 1$ ordinary diode

$= 2\tau/\tau_R$ photoconductor

Note that the transit and recombination time factors affect the shot and generation-recombination noise but not the thermal noise.

The mean square signal and noise voltages appearing across the load resistors R_L in the equivalent circuits are written and compared to obtain the signal-to-noise ratio of the detector. The results are

$$S = \overline{v_s^2(\omega)} = \frac{1}{2} e^2 \eta^2 M^2 F_{so}^2 \left|S(\omega)\right|^2 \left|Z(\omega)\right|^2 \Delta f$$

$$N = \overline{v_n^2} = \left\{ 2e \left[I_i M_n + e\eta M M_n (F_B + F_{Lo} + F_{so}) \right] |S(\omega)|^2 + 4kT/R_p \right\} |Z(\omega)|^2 \Delta f$$

$Z(\omega) = R_p (1 + j\omega CR_p)^{-1}$ where $R_p = RR_L(R + R_L)$. R is the detector resistance; R_L is the load resistor and C is the sum of all shunt capacities in the input network. Δf is a small frequency interval centered around $f = \omega/2\pi$, the signal frequency. The shunt capacity C is the sum of detector capacity and circuit capacity. For diodes, their own capacitance, even for very fast detectors, will usually be at least several picofarads. For photoconductors, this capacitance is predominantly that of the input circuitry.

Normally in very high frequency, wide bandwidth operation R_L, the load resistance or equivalent amplifier input resistance, will be small – of the order of 50Ω. Except for very poor detectors with large internal currents I_i, the thermal noise term $4kT/R_p$ will be larger than the shot or g-r term. In this condition the optimum signal-to-noise ratio results when maximum signal power transfer to the load takes place.

The minimum detectable photon flux in this thermal-noise-limited condition is given for narrow bandwidths by

$$F_{so,\ min} = \frac{(8kT/R_p)^{1/2}}{e\eta M} (\Delta f)^{1/2}$$

If the operating bandwidth is taken as the effective noise bandwidth, determined from the impedance function $Z(\omega) = R_p (1 + j\omega R_p C)^{-1}$ by the relation

$$B = R_p^{-2} \int_0^\infty |Z(\omega)|^2 \, df = (4R_p C)^{-1}$$

then the minimum detectable photon flux in this bandwidth is

$$F_{so,\ min} = \frac{4(2kTC)^{1/2} B}{e\eta M}$$

and the detectivity for signals at optical frequency ν is

$$D = \frac{e\eta M}{h\nu} \frac{1}{4(2kTC)^{1/2} B}$$

DETECTION LIMITS OF SOLID STATE DETECTORS

Considering the other extreme of low frequency, narrow bandwidth operation, where $R_p = (4BC)^{-1}$ can be large, it is possible to reach a bandwidth region where the shot or g-r noise term dominates. For simple direct detection $F_{Lo} = 0$ and, in the case of a good detector for which the internal currents are negligible, the signal-to-noise ratio will be given by

$$\frac{S}{N} = \frac{\overline{v_s^2}}{\overline{v_n^2}} = \frac{\eta M F_{so}^2}{4M_n(F_B + F_{so})\,\Delta f}$$

and the minimum detectable photon flux is given by

$$F_{so,\,min} = \left(\frac{2M_n F_B B}{\eta M}\right)^{1/2} = \frac{1}{h\nu D}$$

which is seen to vary with the square root of the bandwidth B. The transition from the low pass-band shot or g-r noise limited condition to the thermal noise limited condition occurs when the shunt resistance R_p has value

$$R_p = \frac{2kT}{e^2 \eta M\, M_n(F_B + F_{so})}$$

The pass-band at which the change from shot to thermal noise limited performance takes place is

$$B = \frac{e^2 \eta M\, M_n\, F_B}{8kTC}$$

The goal of detector development is to depress the thermal noise portion of the curve so that the shot or g-r noise determined minimum detectable signal can be realized over any desired pass-band.

From the expressions for S and N given earlier, it is apparent that if the signal term and the photon-generated current noise term could be amplified, shot and g-r noise limited performance would be obtained for smaller values of R_p, i.e., over wider pass-bands, B. The techniques which have been suggested for accomplishing this in the case of incoherent detection include (1) high frequency parametric amplification in the photodiode; (2) building diodes in which internal gain is achieved by charge carrier multiplication caused by impact ionization; (3) making the photocurrent gain ratio τ/τ_R greater than 1 in photoconductors.

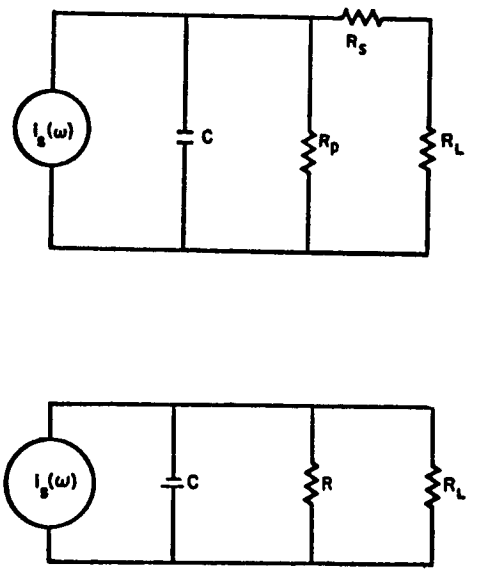

Figure A. Constant Current Equivalent Circuits of the Photodiode (Upper) and Photoconductor (Lower)

DETECTION LIMITS OF SOLID STATE DETECTORS

Heterodyne operation of a detector provides a very effective means of achieving shot and g-r noise limited performance and, when sufficient local oscillator power can be applied, may even render background contributions to the noise megligible so that a signal fluctuation limit is reached. The expression for the signal-to-noise ratio in this case becomes

$$\frac{S}{N} = \frac{2e^2\eta^2M^2F_{so}F_{Lo}S^2}{\Delta f\left\{4e^2\eta M\, M_n\,(F_B + F_{Lo})S^2 + 4kT/R_p\right\}}$$

For F_{Lo} sufficiently large the only term of significance in the denominator is

$$4e^2\eta M\, M_n F_{Lo} S^2 ,$$

and S/N is simply

$$\frac{S}{N} = \frac{\eta M F_{so}}{2M_n \Delta f}$$

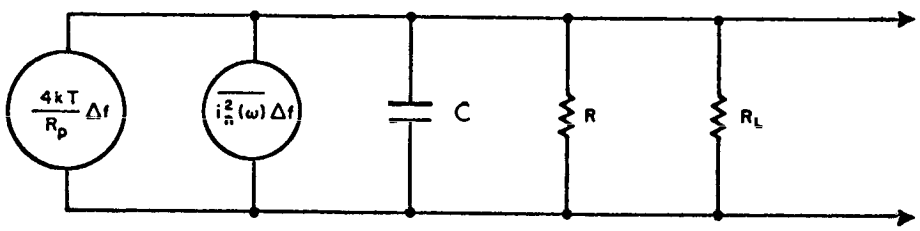

Figure B. Noise Equivalent Circuit for the Photodiode and Photoconductor

$\overline{v_R}^2\ \Delta f$ represents excess noise arising in the preamplifier and has been neglected in the text.

PERFORMANCE OF PHOTOEMISSIVE DETECTORS

Detail Performance Characteristics are given for available photoemissive detectors at the frequencies for ruby, helium-neon, neodymium, and neon lasers.

The following discussion will be devoted to presenting detail on available photomultipliers at several available laser wavelengths.

The following four wavelengths are particularly important in laser technology for the visible and near visible part of the spectrum: 6328 Å, 6943 Å, 1.06μ, and 1.13μ. These are the wavelengths of helium-neon, ruby, neodymium, and neon lasers, respectively. Table A contains quantum efficiencies and relative responsivities of the photosurfaces S-1, -10, -17, and -20 at these important frequencies. * Clearly only the S-1 surface is suitable for 1.06 and 1.13 radiation, and the S-17 surface is inferior to the others at the two shorter wavelengths.

A number of photomultiplier tubes are available with these surfaces. The responsivity and the noise equivalent input of the photomultipliers are usually given in microamperes per lumen** and in lumens. A test lamp of color temperature 2870°K is employed in place of a monochromatic source to determine responsivity and NEP. The values of NEP are given in Table B.

The absolute responsivity of a photomultiplier depends on the voltages applied to its dynodes. The manufacturers usually state the responsivity under specified conditions in microamperes per lumen, the source of irradiation being a black body at 2870°K temperature. The calculation of the signal-to-noise ratio is based on the NEP of Table B plus the shot noise plus other noise that may be entering the detector with the signal, including the noise due to signal fluctuations.

D. Gunter, et al., have reported signal enhancement in photomultipliers by factors as large as four by making use of multiple reflection in the glass face of the tube on which the photocathode is deposited. They added a glass quadrant to the tube and noted that when the angle of incidence increases above that characteristic of total internal reflection the response increased a factor of 4 in the red and 2 in the blue.

---

*See topic entitled "Theory of Photomultiplier Detectors" for optical frequency response of these detectors.

**1 lumen = 1.496×10^{-3} watts, at max visibility, $\lambda = 5560$ Å.

Table A. Quantum Efficiencies and Responsivities of Red-Sensitivity Photosurfaces

	6328 Å		6934 Å		1.06μ		1.13μ	
Photo-surface	Quantum Efficiency	Respon-sivity	Quantum Efficiency	Respon-sivity	Quantum Efficiency	Respon-sivity	Quantum Efficiency	Respon-sivity
S-1	0.0033	0.56	0.0040	0.80	0.0009	0.29	0.00016	0.03
S-10	0.0070	0.30	0.0028	0.10	0	0	0	0
S-17	0.0080	0.08	0.0004	0.017	0	0	0	0
S-20	0.045	0.41	0.028	0.22	0	0	0	0

Table B. NEP in One-Cycle Band at 6328 Å and 6943 Å for Several Photomultipliers

Tube	NEP, $W\text{-}sec^{-1/2}$		Temperature, °C
	6328 Å	6943 Å	
7102	3.0×10^{-12}	2.1×10^{-12}	25
6217	2.6×10^{-13}	7.9×10^{-13}	25
7265	4.3×10^{-15}	8.0×10^{-15}	25
7265	5.6×10^{-16}	10.4×10^{-16}	-80
7326	1.07×10^{-14}	2.0×10^{-14}	25
7326	1.6×10^{-15}	3.2×10^{-15}	-80

For $\lambda = 1.06\ \mu$ the NEP of the 7102 tube is 5.9×10^{-12} $W\text{-}sec^{-1/2}$.
For $\lambda = 1.13\ \mu$ it is 5.7×10^{-11} $W\text{-}sec^{-1/2}$.

DETECTORS FOR 10.6 MICRONS

Five solid state detectors can be considered for detection of 10.6μ energy. Of these copper doped germanium is preferred.

Five semiconductor materials can be considered for the detector in a 10.6μ laser system. These materials, with their characteristics cutoff wavelength and maximum operating temperature, are listed in the Table. Spectral response curves and plots of the temperature variation of detectivity for several of these materials are shown in Figures A and B, respectively.

The first four semiconductor materials in the Table are extrinsic (impurity) photoconductors. The acceptor impurity concentrations for these materials are typically $2\text{-}3 \times 10^{14}$ cm^{-3} for cadmium, $2\text{-}3 \times 10^{15}$ cm^{-3} for mercury and gold, and $1\text{-}2 \times 10^{16}$ cm^{-3} for copper. Above the critical temperature T_{max}, carriers are produced by thermal ionization of these impurity centers and carrier concentration increases exponentially with temperature. Below this critical temperature the concentration of carriers in the semiconductor is determined by the magnitude of the background radiation, and the detector is defined as operating in the background limited photoconductivity condition. The upper limit of detectivity (D*) is set by the level of background radiation on the detector and the quantum efficiency. Above the critical temperature in the region of thermal ionization, the detectivity decreases exponentially with temperature.

Of the three extrinsic materials listed in the Table, Ge:Cu is preferred for many applications for the following reasons:

1. Ge:Cu is the easiest to prepare since the copper is introduced by solid state diffusion. Copper has a very high diffusion coefficient in germanium. (Conversely Ge:Hg and Ge:Cd are prepared by horizontal zone leveling under a high vapor pressure of the constituent impurity.)

2. The higher impurity concentrations possible in Ge:Cu produce a high absorption coefficient and permit higher quantum efficiencies in a smaller sample thickness.

3. In general, Ge:Cu detector samples exhibit a lower resistance than either Ge:Hg or Ge:Cd. This factor is a distinct advantage in designing a detector for very high frequencies where a low RC time constant is mandatory.

The chief disadvantage of the copper-doped germanium detector is the requirement for a very low operating temperature, i.e., liquid helium cooling. In closed cycle cooling a two-stage Stirling cycle cooler is necessary. The mercury-doped germanium detector has the major advantage of operation at temperatures up to about twice the absolute maximum temperature allowed for Ge:Cu. From the practical point of view, operation at liquid hydrogen and liquid neon temperature, as well as liquid helium, represents a distinct advantage. The use of single stage Stirling cycle refrigeration is an additional advantage when closed cycle cooling is desired. Ge:Au operates at the highest temperature of

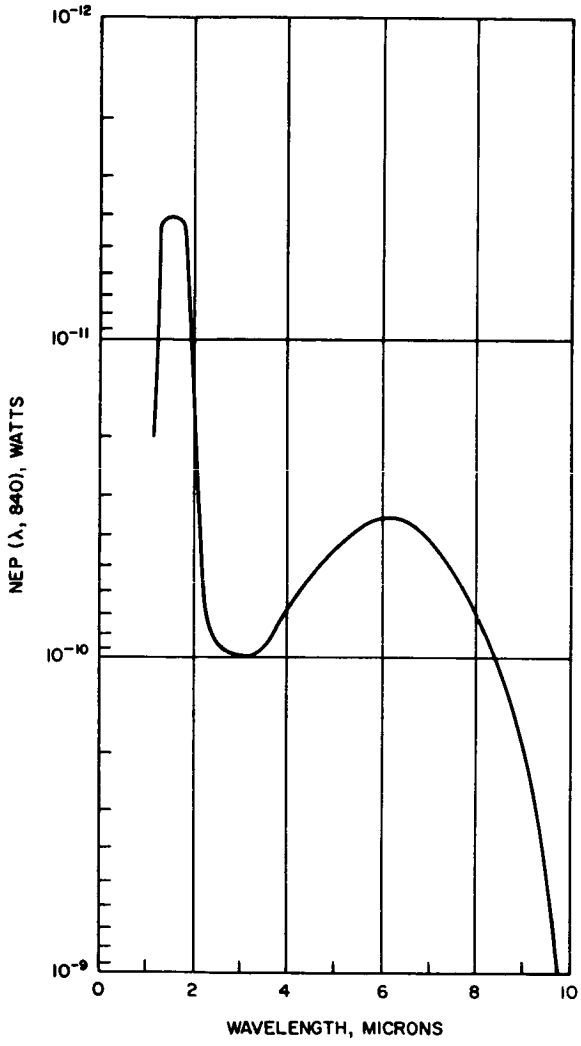

1. Gold-doped germanium.

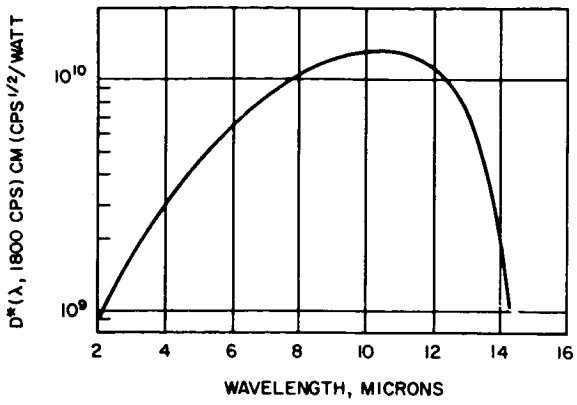

2. Mercury-doped germanium.

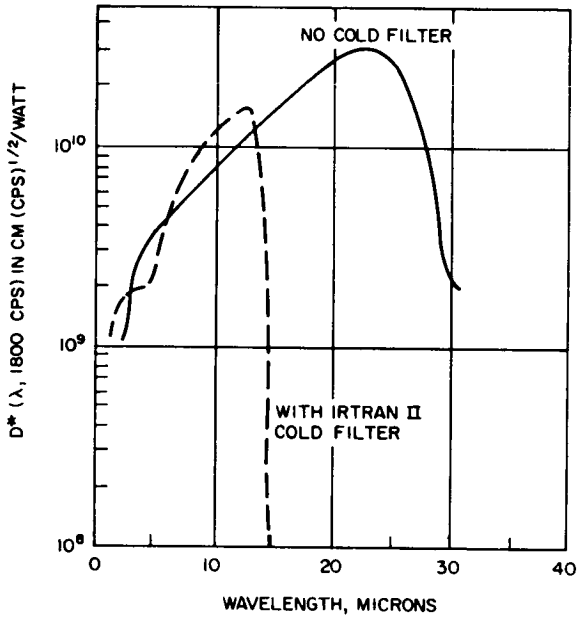

3. Copper-doped germanium.

Figure A. Monochromatic Detectivity as a Function of Wavelength for Several Extrinsic Photoconductors

DETECTORS FOR 10.6 MICRONS

all the extrinsic photoconductors and can even be used at 77°K (liquid nitrogen). However, at this temperature its detectivity is a factor of two less than its peak value. Also, its detectivity at 10μ is two orders of magnitude less than its peak value. Preliminary results of measurements of the frequency response of especially compensated mercury- and copper-doped germanium detectors[1] manufactured by the Santa Barbara Research Center indicate they exhibit a flat frequency response up to 300 MHz. From this it is concluded that the inherent lifetime of these materials is less than 5×10^{-10} seconds.

The last material listed in the Table ($Hg_{1-x}Cd_xTe$) is an intrinsic semiconductor. This material currently is just emerging from the status of a laboratory curiosity. The yield of good material with proper composition and purity has been very low, but research efforts at a number of laboratories are gradually solving some of these problems. As technology advances and the yield improves, this particular material offers great promise for operation to 12μ at liquid nitrogen temperature (77°K).

Characteristics of Semiconductor Materials for 10.6μ Detector

Detector Material	$\lambda^{1/2}$, μ [a]	T_{max}, °K [b]
Ge:Au	~9	70
Ge:Hg	14	40
Ge:Cd	22	25
Ge:Cu	28	18
$Hg_{1-x}Cd_xTe$	12	77

[a] Wavelength at which detectivity decreases to 1/2 its peak value.

[b] Temperature at which detectivity decreases to $1/\sqrt{2}$ of its maximum value.

[1] Picus, G. S., Interim Technical Report No. 2 Contract AF33(615)-3847, Hughes Research Laboratories, Malibu, California.

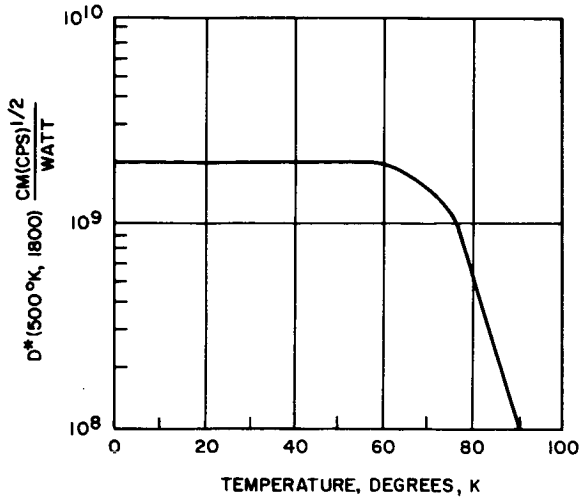

a. Gold-doped germanium.

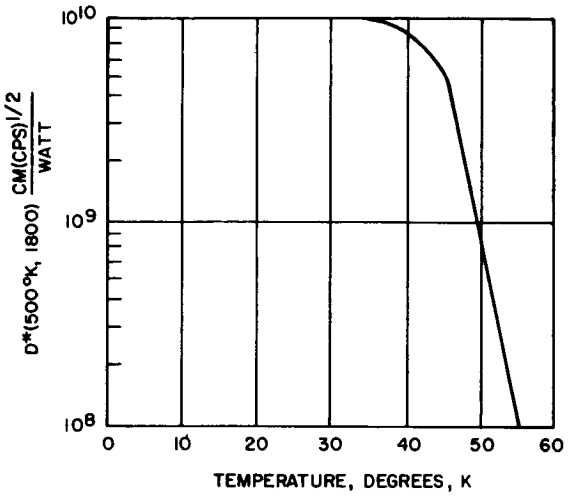

b. Mercury-doped germanium.

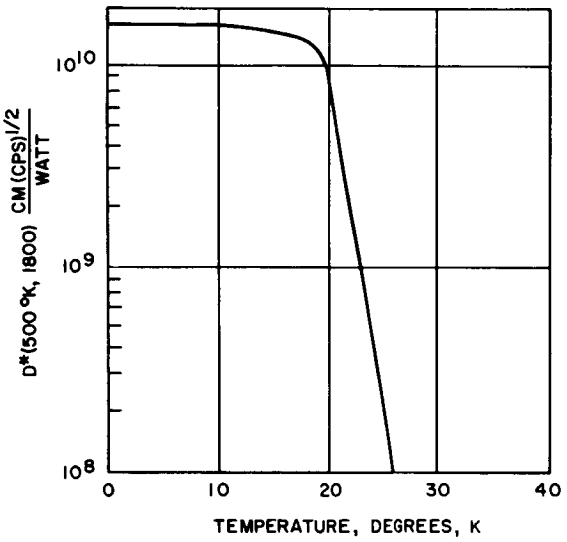

c. Copper-doped germanium.

Figure B. Blackbody Detectivity as a Function of Temperature for Several Extrinsic Photoconductors

DETECTOR PERFORMANCE SUMMARY

A summary of detector detectivity is given which spans wavelengths of 0.1 micron to 40 microns.

A summary of detector performance is given in the Figure. This material was first published in ASD-TDR-63-185, "Investigation of Optical Spectral Regions for Space Communications." May 1963, AF Avionics Laboratory, Wright-Patterson AFB, Ohio. (Unclassified)

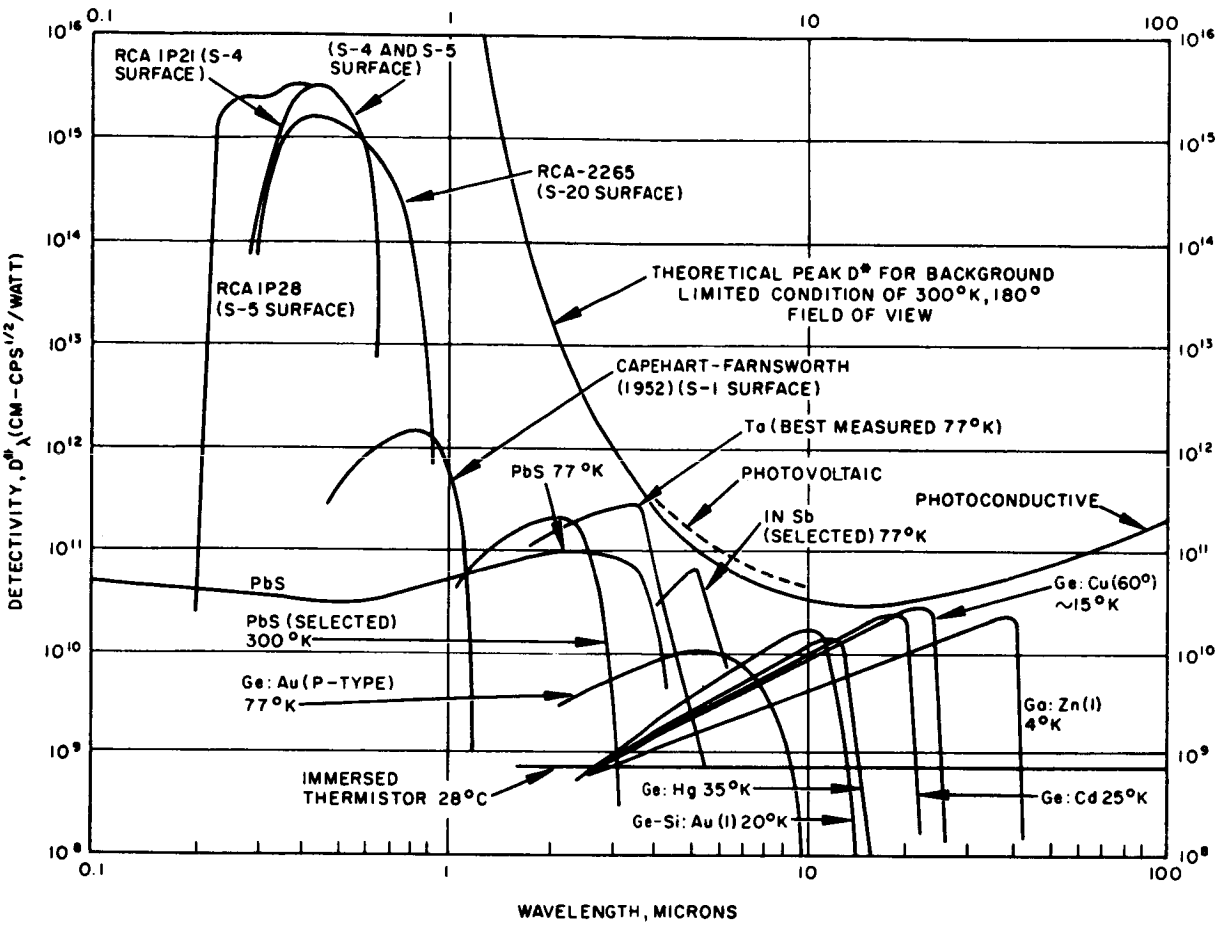

Detectivity versus Wavelength for the Best Detectors

BURDENS FOR OPTICAL FREQUENCY DETECTORS

Burdens of weight, cost, and input power requirements are given for optical demodulations, which include the detector. The total demodulator also includes the circuitry required to produce a noise free (but not necessarily error free) bit stream.

A complete description of a detector must cover the following three areas in order to be useful to the systems designer.

1. The optical configuration—this means the physical size and shape of the detector and its housing and the extent to which these can be modified. These properties are important in the selection and design of both system optics and electronics.

2. The electrical configuration—the most important feature here is the characterization of the detector as an active circuit element. This information is required in order to calculate the electrical signal delivered to the electronics as a function of the radiation signal input and in order to investigate the noise performance of the detector and its associated receiver.

3. The support configuration—included in this area are such factors as the electrical bias required to make the detector operative, cooling requirements, and, in the case of heterodyne systems, the local oscillator requirement.

The electrical configuration has been described in some detail in the previous topics. It is the purpose of this topic to present general relationships between the bit rate (bits per second) detected by the detector and the weight, cost, and power required by the entire demodulator assembly.

These relationships are given in Figures A, B, and C. As expected the more complicated detection system, heterodyne detection, requires the most weight and power and is the highest cost system.

The curves of Figures A, B, and C provide the demodulator representation needed by the Optimization Methodology described in Volume II, Part 1. The values given in the Figures are for representative sample configurations, detailed designs will undoubtedly modify these values.

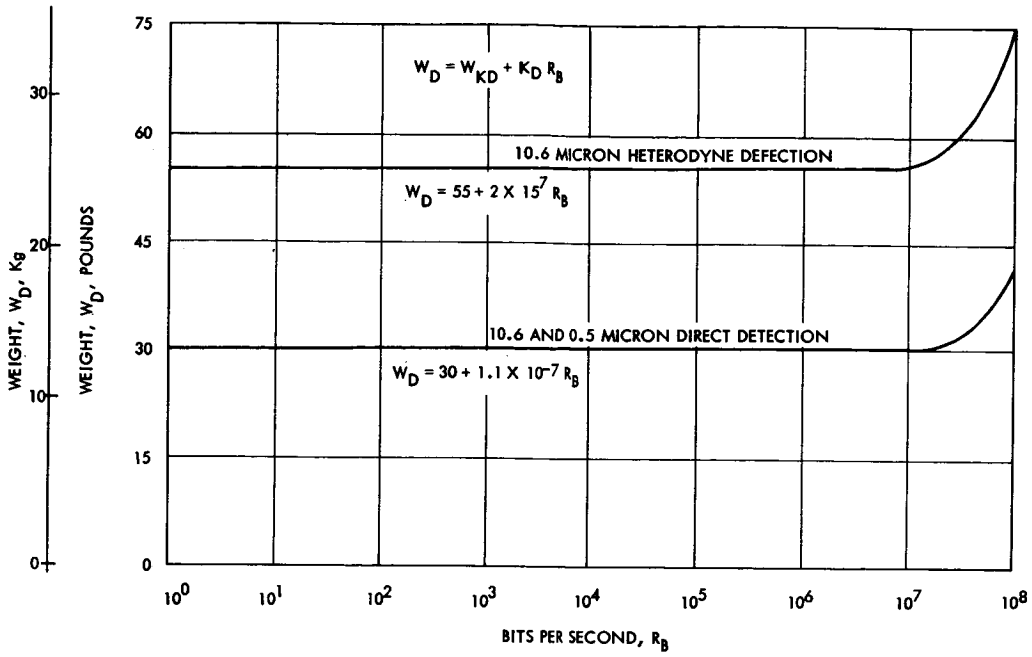

Figure A. Demodulator Weight

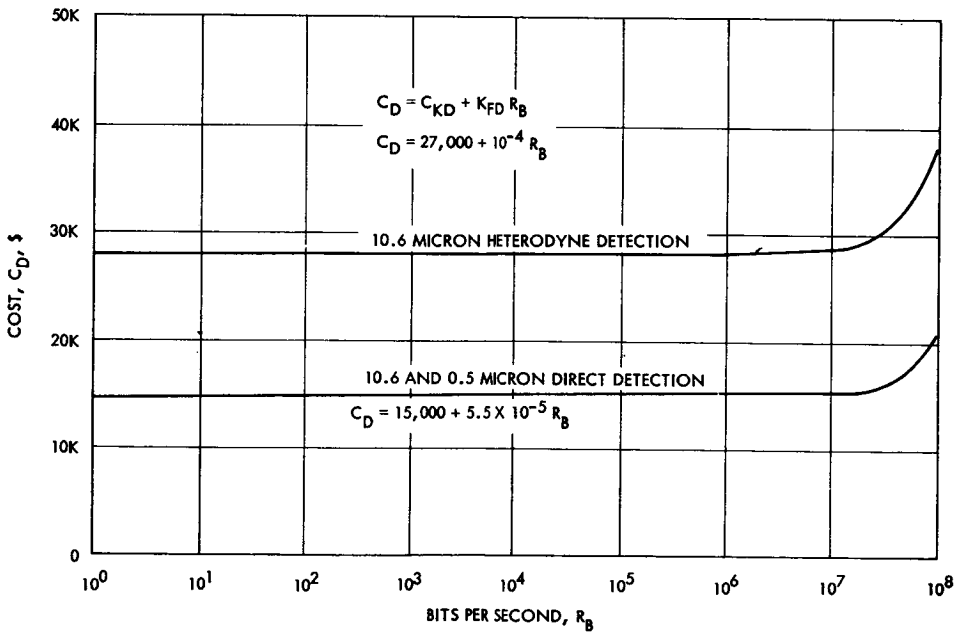

Figure B. Demodulator Cost

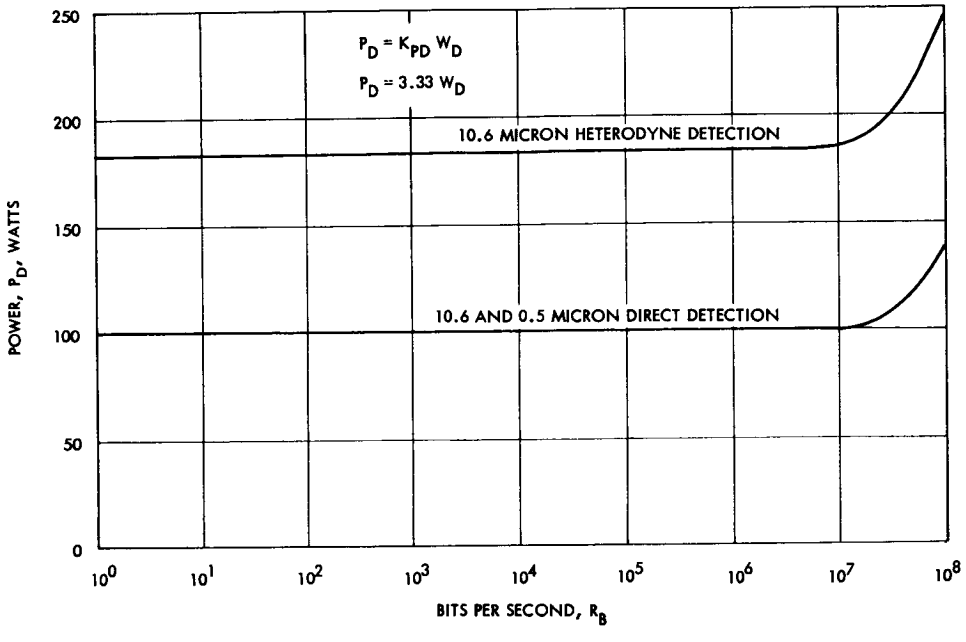

Figure C. Demodulator Power